Exploring cloudy gas accretion as a source of interstellar turbulence in the outskirts of disks

A. Santillán[1], F.J. Sánchez-Salcedo[2] and J. Franco[2]

ABSTRACT

High–resolution 2D–MHD numerical simulations have been carried out to investigate the effects of continuing infall of clumpy gas in extended H I galactic disks. Given a certain accretion rate, the response of the disk depends on its surface gas density and temperature. For Galactic conditions at a galactocentric distance of ~ 20 kpc, and for mass accretion rates consistent with current empirical and theoretical determinations in the Milky Way, the rain of compact high velocity clouds onto the disk can maintain transonic turbulent motions in the warm phase (~ 2500 K) of H I. Hence, the H I line width is expected to be ~ 6.5 km s^{-1} for a gas layer at 2500 K, if infall were the only mechanism of driving turbulence. Some statistical properties of the resulting forcing flow are shown in this Letter. The radial dependence of the gas velocity dispersion is also discussed.

Subject headings: galaxies: intergalactic medium — galaxies: ISM — hydrodynamics — ISM: kinematics and dynamics — ISM: structure — turbulence

1. Introduction

H I line widths, σ_W, are observed to vary from ~ 12 to 15 km s^{-1} in the central parts to 6-8 km s^{-1} in the outer parts. Beyond the optical disk, the maps of σ_W display a patchy distribution with values populating the interval from 5 to 9 km s^{-1}, independent of galactocentric distance. The median value is fairly constant along the extended outer parts, with about the same universal value 7 ± 1 km s^{-1} for all the observed galaxies (Lewis 1984; Dib, Bell & Burkert 2006, and references therein). By fitting two-component Gaussians to

[1]Cómputo Aplicado-DGSCA, Universidad Nacional Autónoma de México, Ciudad Universitaria, 04510 Mexico City, Mexico; alfredo@astroscu.unam.mx.

[2]Instituto de Astronomía, Universidad Nacional Autónoma de México, Ciudad Universitaria, 04510 Mexico City, Mexico; jsanchez@astroscu.unam.mx, pepe@astroscu.unam.mx.

the H I profiles in NGC 6822, the second-moments for the cold and warm phases of the H I were found to be $\sigma_W \approx 5$ km s^{-1} and $\sigma_W \approx 8$ km s^{-1}, respectively (de Blok & Walter 2006).

The observed σ_W are likely to represent turbulent small-scale motions: the existence of a cold phase in the outer disks, the observed level of star formation and the double exponential radial profile of the star formation rate have been also interpreted as a consequence of the turbulence gas compressions in the outer disks (e.g., Ferguson et al. 1998; Elmegreen & Hunter 2006).

Dib, Bell & Burkert (2006) found that if turbulence is driven by supernova, the velocity dispersion of the H I gas in the quiescent regime is ~ 3 km s^{-1}, a factor of ~ 2 smaller than the observed values. Thus, either there are other physical processes driving turbulence or the supernova feedback efficiency has been underestimated. There exist several physical mechanisms that could drive turbulence even in the absence of star formation: hydrodynamic or magnetohydrodynamic instabilities, frequent minor mergers of small satellite clumps, ram pressure or infalling gas clouds. Amongst the hydrodynamical instabilities, the thermal instability by itself cannot sustain turbulence (Sánchez-Salcedo 2001; Gazol et al. 2001; Brandenburg, Korpi & Mee 2007). The magnetorotational instability, on the other hand, can only account for an amount of turbulent motions ~ 4.5 km s^{-1} for the three components, if thermal broadening is not subtracted, and might be completely suppressed by stellar feedback (Dib et al. 2006 and references therein).

Our main goal is to assess how much of the velocity dispersion observed in the ISM can be due to the impact of high velocity clouds (HVCs) and intermediate velocity clouds (IVCs). Ample evidence for the presence of continuing gaseous infall to the Galactic disk has been compiled in Beckman et al. (2003). All the studies firmly suggest that the inflow in the Galactic disk has been constant, with an accretion rate of ~ 1 M$_\odot$ yr^{-1}, or has even increased, during its lifetime. H I observations have revealed accretion of both diffuse and discrete structures from the extended environment in M31 and M33 (Thilker et al. 2004; Braun & Thilker 2004). Putman (2006) infers that the present total mass in condensed infalling clouds around the Milky Way is $\sim 6 \times 10^8$ M$_\odot$ if they are all at distances < 60 kpc. HVCs may be a repository for large amounts of gas if clouds fall into the disk rapidly after they are formed (Maloney & Putman 2003; Maller & Bullock 2004; Putman 2006). In the next sections, we consider the turbulent H I dynamics driven by the infall of clouds. Preliminary results were reported in Sánchez-Salcedo et al. (2007).

2. The model

The ideal MHD equations are integrated using the ZEUS code (Stone & Norman 1992a,b). A local Cartesian frame of reference with x and z corresponding to the horizontal and vertical directions, respectively, was adopted to simulate a small patch of our Galaxy at a distance R_0 from the Galactic center. The galactic symmetry plane, $z = 0$, is placed in the middle of the computational domain. The simulation domain is a square of size $L \times L$ with 1024^2 zones. The ambient medium that is interacting with the HVCs is initially in plane-parallel magnetohydrostatic equilibrium with scaleheight h_0 in an external gravitational potential. Here the scaleheight is defined as half width at half maximum of the vertical volume density of the gas layer. The ambient gas is initially isothermal in space with *thermal* sound speed c_s and its evolution is nearly isothermal with specific heat ratio $\gamma = 1.01$. Gas self-gravity was disregarded. The magnetic field has only one component along the y–axis and is initially stratified in the z–direction, $B_{\rm y}(z)$. Thus, there is no magnetic tension, only magnetic compression. Two magnetic configurations are explored. The first one is the high-latitude extension of the Galactic thick disk of Boulares & Cox (1990, BC model hereafter) following Santillán et al. (1999). The vertical gravitational force and the magnetic field configuration were scaled to the outer Galaxy, neglecting edge effects. The second set of models assumes that B_y^2 falls off with the gas density (Spitzer case) in the initial equilibrium configuration, so that α, defined as the ratio between the magnetic and thermal pressure, is constant. In all the simulations, the size of the domain is $L > 10h_0$ in order to avoid spurious boundary effects. We apply periodic boundary conditions in the x–axis, and open boundary conditions on the upper and lower faces of the computational domain.

The too low thermal gas pressure at the outer parts of extended galactic disks will permit only the warm (several times 10^3 K) phase of H I to exist (e.g., Elmegreen & Parravano 1994). Heiles (2001) provides observational evidence that about half of the mass of the diffuse gas in the Galaxy may have temperatures from a few hundred to a few thousand kelvin. In this work, we will explore c_s values in the range 4.5–8 km s^{-1}.

The ambient gas is subject to a continuous rain of HVCs. In most simulations, if not specified otherwise, all the clouds with initial radius R_{cl} and uniform internal density n_{cl}, are injected at $z = z_{cl}$ with a vertical velocity v_{cl}, and are placed randomly in x. We found that the statistical properties of the flow in the disk are similar when the injection occurs along both caps $z = \pm z_{cl}$.

The remaining five dimensionless parameters that characterize our simulation models are $\alpha(z)$, R_{cl}/h_0, v_{cl}/c_s, n_{cl}/n_0, and $\lambda_{\rm acc}$, where n_0 is the midplane volume density at $t = 0$ and $\lambda_{\rm acc}$ is the fraction of accreted mass in one sound crossing time, $\lambda_{\rm acc} \equiv (h_0/c_s)\,(\dot{\Sigma}/\Sigma_i)$

with Σ_i is the initial column density of the disk. Note that once c_s is fixed, the scaleheight h_0 is determined by the depth of the external gravitational potential. The collisions of infalling clouds onto the gaseous disk will take the gas out of hydrostatic equilibrium. Consequently, the scaleheight h of the H I layer may evolve in time.

3. Results

The disk gas is subject to a stocastic driving force caused by the MHD pull of randomly-injected clouds, plus the restoring gravitational force which tends to push back the gas to the midplane. The level of substructure in the resulting fluid depends on the structural parameters of the clouds and injection velocity. We focus first on describing the evolution of our fiducial BC model, labelled as run BCa, that is intended to represent conditions at a galactocentric distance $R_0 = 20$ kpc. In this model, the parameters of the disk are $c_s = 8$ km s^{-1}, $\Sigma \simeq 1.2$ M$_\odot$ pc^{-2} and $h_0 = 220$ pc. For the clouds we adopted $v_{cl} = 100$ km s^{-1}, $z_{cl} = 2$ kpc, $n_{cl} = 0.1$ cm^{-3} and $R_{cl} = 50$ pc (see Sánchez-Salcedo et al. 2007 for a discussion of this choice). The injection rate of clouds in the whole box domain is 300 per Gyr, corresponding to an accretion rate defined as $4\pi R_0^2 \dot{\Sigma}$ of 0.6 M$_\odot$ yr^{-1}. While our simulations are 2D, this situation is energetically equivalent to an accretion rate of 750 clouds per Gyr and per kpc^2 of galactic disk. Since the kinetic energy of a cloud is $\sim 10^{50}$ erg, the energy input rate from impacting clouds is 7.5×10^{52} erg Gyr^{-1} kpc^{-2}, which is equivalent to $75\epsilon^{-1}$ supernova explosions per Gyr and kpc^2 of disk, each with mechanical energy $\epsilon \times 10^{51}$ erg, where $\epsilon \sim 0.1$ is the efficiency factor. At the end of the simulation (2 Gyr), the total mass in our grid increased by a factor 1.45.

Clouds interact with the ambient medium and dilute (see Fig.1). At a height of 500 pc they lose their identity and mix up with the turbulent disk. Hence the number of 'active' clouds is 300 Gyr^{-1} $\times$ (1.5 kpc/100 km s^{-1}) $\sim$ 4–5. The infalling clumpy flow perturbs the disk through MHD waves that interact in a complicated fashion, producing a network of plumes and shells (see Fig. 1). As a consequence, the 1D rms velocity of the gas, σ, increases in time and saturates after 100 Myr, reaching values that oscillate between 6 and 7.5 km s^{-1} around the mean value $\bar{\sigma}$ (see Fig. 2). The difference between $\bar{\sigma}_x$ and $\bar{\sigma}_z$ is only ~ 0.5 km s^{-1}. The velocity dispersion in each direction was obtained by fitting the mass-weighted velocity profile for cells within $|z| < h_f$, with h_f the asymptotic value of the scaleheight. Examples of mass-weighted velocity profiles are given in Figure 2b,c. Remind that $\sigma_W = (\sigma^2 + c_s^2)^{1/2}$ for isothermal gas, thus, $\sigma_W \sim 10$ km s^{-1}. For $v_{cl} = 50$ km s^{-1}, σ_x and σ_z reach similar values as in the case $v_{cl} = 100$ km s^{-1}. These results suggest that continuous accretion of a clumpy gas may contribute significantly to the random motions observed.

The vertical density profile averaged on horizontal cuts is shown in Fig. 3, Note that even though the injection of clouds occurs only through the upper cap $z = z_{cl}$, the density profile is quite symmetric and the net vertical displacement is relatively small. The scaleheight is ~ 640 pc at ~ 2 Gyr, similar to the observed value at $R = 20$ kpc.

The injected energy is mostly dissipated in radiative shell compressions and behind shock fronts, being the dissipation timescale for turbulent kinetic energy $\simeq 8$ Myr. The energy spectrum contains information about how the kinetic energy is distributed at different scales and about the nature of the driving mechanisms of the random motions in the compressible ISM. Due to the stratification and the anisotropy of the random motions, we have calculated the power spectrum along horizontal cuts for each component of the velocity separately. The power spectrum follows a power-law with different exponent for each component $E_i(k) \sim k^{-\alpha_i}$, with $\alpha_x = 3$ and $\alpha_z = 4$.

Vázquez-Semadeni (1994) and Padoan, Nordlund & Jones (1997) reported lognormal density probability distribution functions (PDF) for two- and three-dimensional isothermal turbulent flows. We have checked that, in fact, our PDF is approximately lognormal with excesses at large and low densities probably because in our case the turbulence is not isotropic and, in addition, there is some probability of finding density substructure that has not a turbulent origin, it being the remnants of infalling clumps.

When the clouds are randomly injected along both caps, the mass enhancement in the central disk ($|z| < 600$ pc) is slightly larger (about 10%) than when the injection only proceeds along one side, because the symmetry in the injection leads to a more efficient balance of momentum. However, $\sigma(t)$ is quantitatively similar and thus there is no need to show it again.

The elasticity of the disk to collisions depends on the speed of sound and on the magnetic field strength. In order to see the sensitivity of σ on the adopted magnetic configuration, we started with an $\alpha = 1$ Spitzer model and the same c_s and total pressure at the midplane as in run BCa. $\bar{\sigma}_x$ and $\bar{\sigma}_z$ were found to be 5 and 6.2 km s^{-1}, respectively.

It turns out very difficult to infer from basic principles how $\bar{\sigma}$ scales with c_s or with any other parameter (Sánchez-Salcedo et al. 2007). In order to gain some insight, Spitzer configurations with $\alpha = 1$ but different c_s, between 5 and 12 km s^{-1} (spaced by 1 km s^{-1}), were considered. If the total pressure at the midplane $z = 0$ is identical in all the models and equal to the value in the standard model[1], we find that $\bar{\sigma}$ scales linearly with c_s; a good

[1]The fact that the total pressure at $z = 0$ is the same in these models implies that the surface gas density increases for low values of c_s.

fit to the data is $\bar{\sigma}_z = 0.55 c_s + 1.16$ (thermal broadening has been subtracted) when $v_{cl} = 50$ km s^{-1}. If, instead of the total pressure, the surface gas density is taken the same as in the case BCa in all the experiments, then $\bar{\sigma}_z \propto \sqrt{c_s}$. For instance, using again $v_{cl} = 50$ km s^{-1}, $\bar{\sigma}_z$ varies from 7.4 km s^{-1} to 5.0 km s^{-1} when the sound speed drops by a factor of 2 (from 12 km s^{-1} to 6 km s^{-1}).

In order to simulate various galactic conditions at different galactocentric distances, runs have been carried out varying $\lambda_{\rm acc}$ and R_{cl}/h_0. Assuming that R_{cl} does not depend strongly on radius, R_{cl}/h_0 should decrease with R because the observed h increases with R, but it is uncertain as R_{cl} could also increase with R as well. The radial variation of $\lambda_{\rm acc}$ is also uncertain because the accreting mass flux $\dot{\Sigma}(R)$ and the temperature structure $c_s(R)$ should be known. As a departure assumption consider that accretion of an intergalactic plane-parallel flow at infinity occurs ballistically $\dot{\Sigma} \propto R^{-1/2}$ (López-Corredoira et al. 2002). For our Galaxy, Σ decreases by a factor of ~ 10 between 15 and 25 kpc, whereas h increases by a factor of 4. Thus, $\lambda_{\rm acc}$ varies by a factor of ~ 30 assuming that c_s is constant with R. In order to bracket conditions at these galactocentric distances, $\lambda_{\rm acc}$ has been varied by a factor of 25 for run BCb as compared to run BCc, whereas R_{cl}/h_0 varies by a factor of 4 (see Table 1). In runs BCb and Sp-b, σ_z reaches a maximum and decreases afterwards partly because the accreted mass in the disk is no longer negligible in the length of the run. Since in these experiments v_z deviates significantly from a Gaussian distribution, whereas v_x is still well described by a Gaussian, only the values of $\bar{\sigma}_x/c_s$ are reported in Table 1. According to run BCc, which represents Galactic conditions at $R \sim 15$ kpc, we find that for $c_s = 4.5$ km s^{-1}, $\bar{\sigma}_x \approx 3.4$ km s^{-1} and $\sigma_W = 5.6$ km s^{-1} if thermal broadening is taken into account. At $c_s = 8$ km s^{-1}, $\bar{\sigma}_x \approx 4.5$ km s^{-1} (thus $\sigma_W = 9$ km s^{-1}). At the outer far disk (~ 25 kpc), $\bar{\sigma}_x$ is found to be 7.5–10 km s^{-1} for $c_s = 4.5$ and 8 km s^{-1}, respectively ($\sigma_W \sim$ 9–13 km s^{-1}). To derive these values, we rescaled the results of run BCb appropriately using our previous result that $\bar{\sigma}_x \propto \sqrt{c_s}$. Slightly smaller σ's are derived for Spitzer models (see Table 1). Line widths of ~ 10 km s^{-1} as predicted at the edge of the disk seem rather high, but note that empirical determinations are scarce and very uncertain at low surface gas densities ($\Sigma < 1$ M$_\odot$ pc^{-2}) (e.g., Shostak & van der Kruit 1984).

If accretion occurs through rare mergers of very massive clouds, it would be hard to see how such a localized events could produce the observed uniform level of turbulence. Nevertheless, experiments with input rates of new clouds 25 times smaller than in our fiducial simulation (i.e., 12 per Gyr in our box domain) but cloud radii 5 times larger (250 pc in physical units), so that the mass accretion rate is unchanged, still maintain a rather uniform level of turbulence everywhere.

4. Discussion and conclusions

We have shown that rms velocities of 3–8 km s^{-1} in the warm phase of H I naturally arise if outer disks are continuously stirred by a clumpy accretion flow at a rate consistent with observations. The exact radial variation of the H I line width depends on the uncertain contribution of the thermal broadening as a function of radius and on the adopted accreting mass flux $\dot{\Sigma}(R)$, which ultimately depends on which the origin of the condensing clouds is. An interesting possibility is that the outer disk is being rained on by Galactic fountain material driven by inner starbursts (Benjamin & Shapiro 1993) or due to matter circulation in the halo. Under the rather extreme assumption that clouds fall ballistically from infinity, σ_W is expected to vary only $\sim 60\%$ between 1 and 1.7 times the optical radius. The coupling between gas accretion and stellar feedback could account for the uniformity of the H I line widths.

So far, our quasi–isothermal simulations do not capture all the physics of the multiphase ISM to permit a detailed comparison between predictions and observations. Three-dimensional simulations including cooling and heating in thermally bistable medium, plus a spectrum of mass and radius of the clouds are being undertaken. These experiments will allow us to derive the velocity dispersion for each component (cool, warm and hot phases) and compare them with high-resolution H I observations that have been able to identify cool and warm neutral components in the ISM of external galaxies (e.g., de Blok & Walter 2006). The accretion of clumpy gas can induce turbulence-compressed regions and trigger star formation, which should be also included.

It is important to consider other phenomena arising in the present accretion scenario. For instance, if turbulence is driven by oblique accretion flows, a large asymmetry in the scaleheight of the H I disk as that observed between the northern and southern halves of the Milky Way (Levine, Blitz & Heiles 2006) is expected because oblique flows have an azimuthal dependence (see Sánchez-Salcedo 2006). In addition, infalling clouds moving supersonically at the upper warm galactic disk develop optical-emitting shocked regions. At a density of the preshocked gas of 5×10^{-3} cm^{-3}, the face-on Hα surface brightness $(I_\alpha)_\perp$ of a certain shocked region may range between 10 and 32.5 mR for shock velocities of 50 and 100 km s^{-1}, respectively (Raymond 1979). In an edge-on galaxy, the expected surface brightness, on scales of ~ 1.5 kpc, is the result of the contribution of all the shocked regions through the sight line: $I \simeq (3\pi/2) N_{cl} R_{cl}^2 R (I_\alpha)_\perp$, where N_{cl} is the number of clouds per unit volume, in our models $N_{cl} \approx 2.5$–5 kpc^{-3}. At $R = 20$ kpc, $I = 12$–40 mR depending on the shock velocity, implying emission measures $EM \equiv \int n_e^2 dl = 0.03$–0.1 pc cm^{-6}, and assuming gas at 8000 K. While the detection of such a Hα brightness is challenging, extremely deep Hα images of edge-on external galaxies might constrain the form in which galaxies accrete mass.

We thank J. Cantó, A. Hidalgo-Gámez, E. Levine, E. Vázquez-Semadeni and the referee for very useful comments. The numerical calculations were performed in the Computer Center at UNAM. This work has been partially supported from DGAPA–UNAM grant IN104306.

REFERENCES

Beckman, J. E., López-Corredoira, M., Betancort-Rijo, J., Castro-Rodríguez, N., Cardwell, A. 2003, Ap&SS, 284, 747

Benjamin, R. A., & Shapiro, P. R. 1993, in The Evolution of Galaxies and Their Environment, ed. D. J. Hollenbach, H. A. Thronson, & J. M. Shull (Mottett Field, CA: NASA), 338

de Blok, W. J. G., & Walter, F. 2006, AJ, 131, 363

Boulares, A., & Cox, D. P. 1990, ApJ, 365, 544

Brandenburg, A., Korpi, M. J., Mee, A. J. 2007, ApJ, 654, 945

Braun, R., & Thilker, D. A. 2004, A&A, 417, 421

Dib, S., Bell, E., & Burkert, A. 2006, ApJ, 638, 797

Elmegreen, B. G., & Hunter, D. A. 2006, ApJ, 636, 712

Elmegreen, B. G., & Parravano, A. 1994, ApJ, 435, L121

Ferguson, A. M. N., Wyse, R. F. G., Gallagher, J. S., Hunter, D. A. 1998, ApJ, 506, L19

Gazol, A., Vázquez-Semadeni, E., Sánchez-Salcedo, F. J., & Scalo, J. 2001, ApJ, 557, L121

Heiles, C. 2001, ApJ, 551, L105

Levine, E. S., Blitz, L., & Heiles, C. 2006, ApJ, 643, 881

Lewis, B. M. 1984, ApJ, 285, 453

López-Corredoira, M., Betancort-Rijo, J., & Beckman, J. E. 2002, A&A, 386, 169

Maller, A. H., & Bullock, J. S. 2004, MNRAS, 355, 694

Maloney, P. R., & Putman, M. E. 2003, ApJ, 589, 270

Padoan, P., Nordlund, A., & Jones, B. J. T. 1997, MNRAS, 288, 43

Putman, M. E. 2006, ApJ, 645, 1164

Raymond, J. C. 1979, ApJS, 39, 1

Sánchez-Salcedo, F. J. 2001, ApJ, 563, 867

Sánchez-Salcedo, F. J. 2006, MNRAS, 365, 555

Sánchez-Salcedo, F. J., Santillán, A., & Franco J. 2007, New Astronomy Reviews, 51, 104

Santillán, A., Franco, J., Martos, M., & Kim, J. 1999, ApJ, 515, 657

Shostak, G. S., & van der Kruit, P. C. 1984, A&A, 132, 20

Stone, J.M., & Norman, M. L. 1992a, ApJS, 80, 753

Stone, J.M., & Norman, M. L. 1992b, ApJS, 80, 791

Thilker, D. A. et al. 2004, ApJ, 601, L39

Vázquez-Semadeni, E. 1994, ApJ, 423, 681

Table 1. Some relevant runs

Run[a]	v_{cl}/c_s	n_{cl}/n_0	R_{cl}/h_0	$10^2\lambda_{\rm acc}^{\ b}$	$\bar{\sigma}_x/c_s$
BCa	12.5	1	0.23	1.2	0.75
BCb	12.5	1	0.11	6.0	1.25
BCc	12.5	1	0.46	0.24	0.56
BCd	12.5	0.1	0.23	1.2	0.25
BCe	1.25	1	0.23	1.2	0.69
Sp-a	8.33	0.9	0.17	2.2	0.70
Sp-b	8.33	0.9	0.17	11.55	1.05

[a] BC refers to the extension of the Boucoulares & Cox (1990) model. Sp indicates that a Spitzer model with $\alpha = 1$ was used.
[b] In physical units, an accretion rate of 0.6 $M_\odot$ yr^{-1} corresponds to 1.2 in the BC model and to 2.2 in the Spitzer model, for the Galactic surface density at 20 kpc.

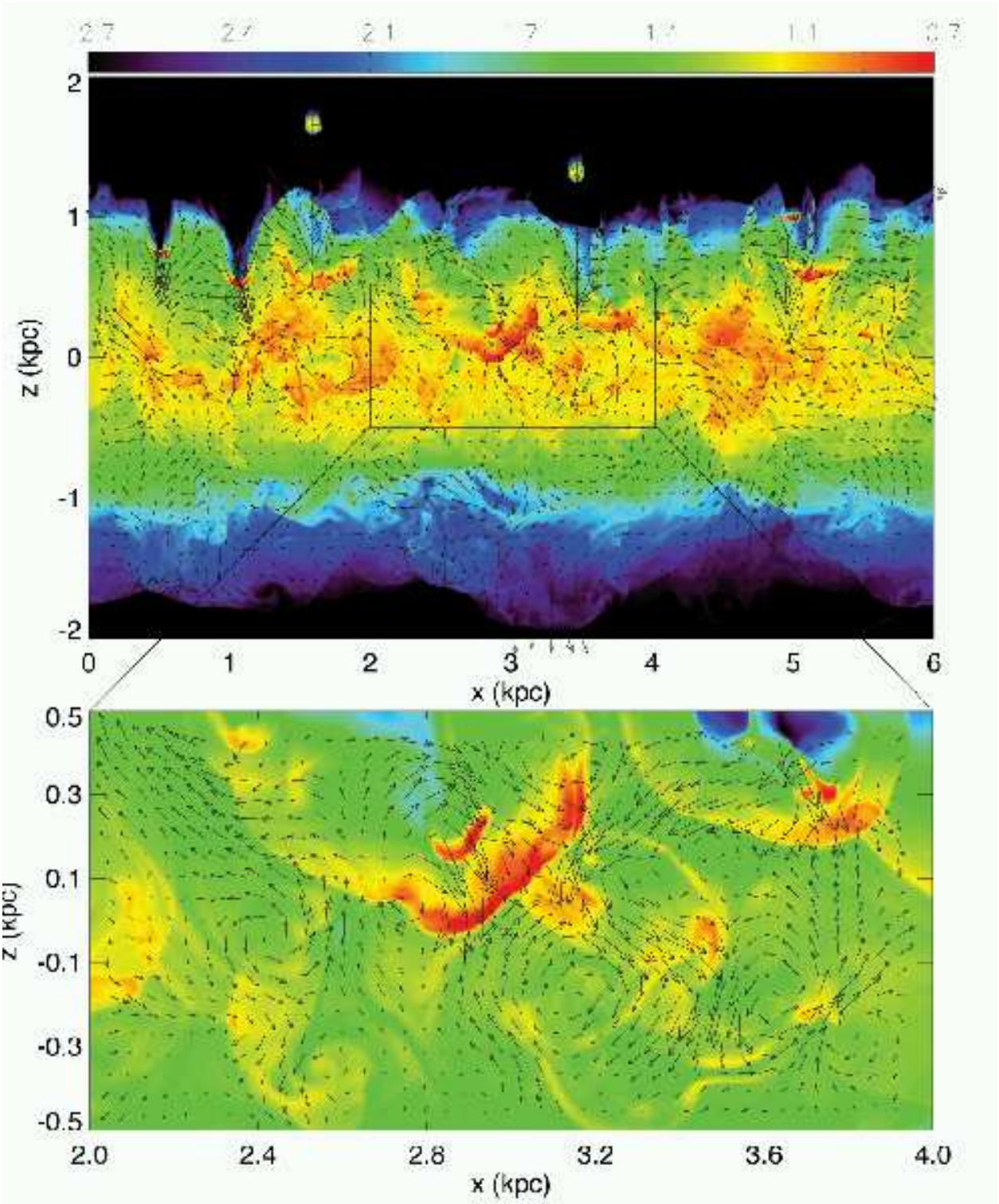

Fig. 1.— Density (*color logarithmic scale*) and velocity field (*arrows*) at $t = 1.7$ Gyr for our run BCa. A general view of the disk between -2 kpc $< z < 2$ kpc (note that the z-axis has been cut-off) is shown (*top*). A magnification zoom right into the marked region is displayed (*bottom*). Notice the presence of vortical motions and the dilution of the infalling clouds.

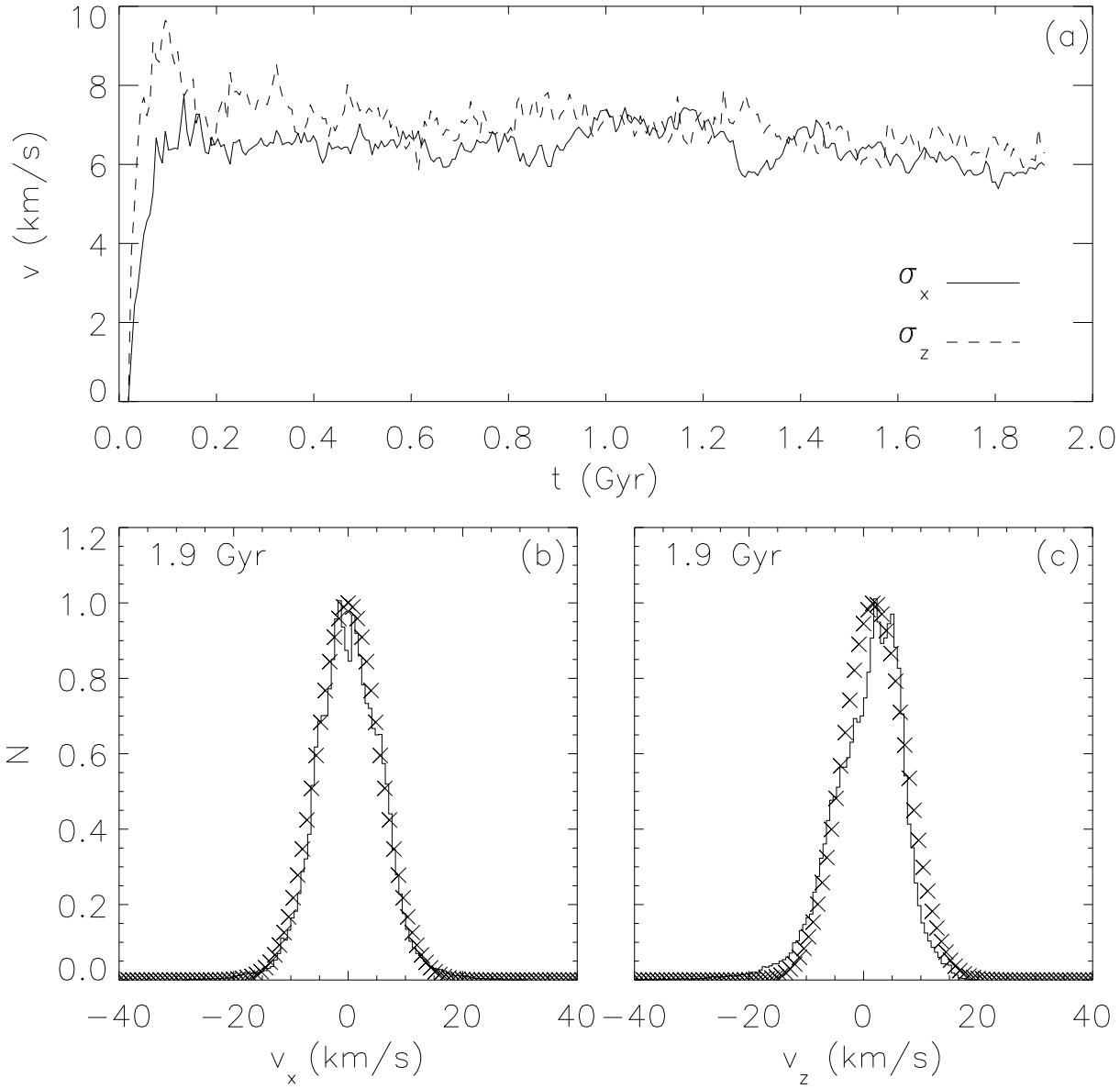

Fig. 2.— Horizontal (*solid line*) and vertical (*dashed line*) velocity dispersions, with thermal broadening subtracted, for our fiducial case (run BCa), as a function of time (panel *a*). Panels *b* and *c* show the mass-weighted profile at $t = 1.9$ Gyr. The profiles sample those gas elements within one scaleheight of the disk. Overplotted are the Gaussian fits (crosses).

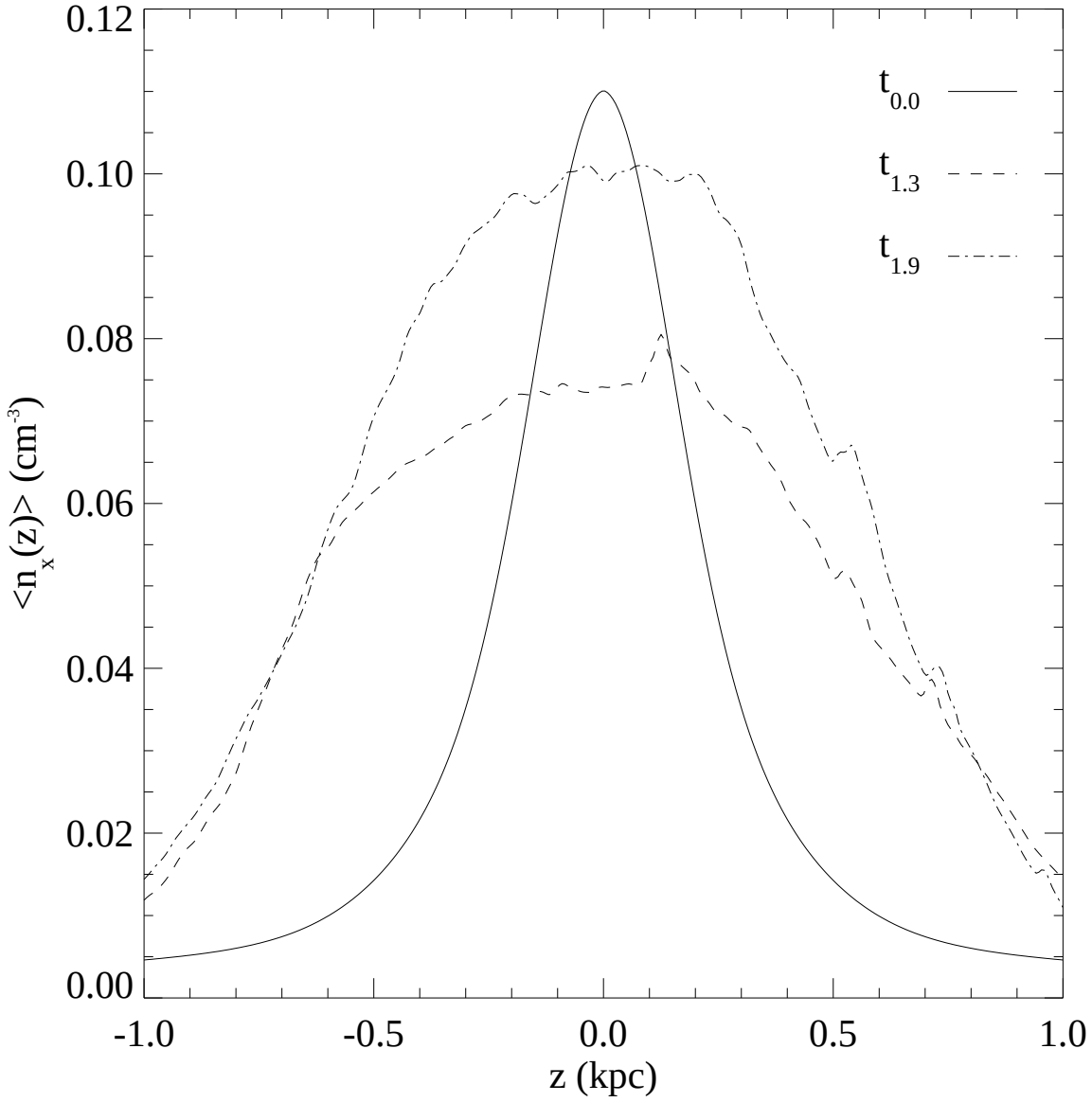

Fig. 3.— The vertical density profile averaged on horizontal cuts is shown at three selected times, $t = 0, 1.27$ and 1.9 Gyr, for run BCa. The corresponding scale heights are 220, 660 and 640 pc, respectively.